Advanced Oxidation Processes of Amoxicillin Based on Visible Light Active Nitrogen-Doped TiO_2 Photocatalyst

Kusuma Putri Suwondo, Nurul Hidayat Aprilita, and Endang Tri Wahyuni*

Department of Chemistry, Faculty of Mathematics and Natural Sciences, Universitas Gadjah Mada, Sekip Utara, Yogyakarta 55281, Indonesia

* ***Corresponding author:***

email: endang_triw@ugm.ac.id

Received: January 17, 2023
Accepted: March 16, 2023

DOI: 10.22146/ijc.81387

Abstract: *Environmental consequences during the COVID-19 pandemic have attracted attention due to the excessive use of antibiotics which lead to the release of the drug's residue, such as amoxicillin (AMX), into the environment. In this work, an advanced oxidation process based on a visible, active N-doped TiO_2 photocatalyst was carried out to eliminate AMX. Nitrogen with different initial doping concentrations (15, 30, 45% w/w) was doped into TiO_2 by the sol-gel method. The characterization technique such as XRD, FTIR, UV-SRS, and SEM-EDX revealed that nitrogen with 30% doping concentration improved the TiO_2 response in the visible region, attributed to the lower band gap energy (2.97 eV). In the photodegradation processes, the TiO_2-N (30%) photocatalyst possessed higher AMX degradation than undoped TiO_2 for both UV and visible light irradiation. In an aqueous solution, the degradation percentage of AMX by TiO_2-N (30%) was 68.5 and 84.12%, while the degradation percentage of AMX by TiO_2 was 38.7 and 78.01% under visible and UV light, respectively.*

Keywords: *antibiotic resistance; visible light active; N-doped TiO_2; amoxicillin*

■ INTRODUCTION

The Coronavirus disease 2019 (COVID-19) has become an outbreak pandemic since 2020. Up to now, 600 million cases worldwide have been reported, causing more than 6 million deaths [1]. The pandemic brought not only a global health crisis but also environmental damage.

The use of pharmaceutical compounds, especially antibiotics, has dramatically increased during the pandemic. Around 75% of COVID-19 patients were prescribed antibiotics to cure or prevent secondary bacterial infection [2]. The ingested antibiotic is mostly excreted through feces and urine because it is poorly metabolized. Hence, their continuous overuse or misuse led to abundant environmental drug residue. The most crucial problem is that antibiotics increase antimicrobial resistance (AMR). The World Health Organization (WHO) declared AMR as a global health crisis problem [3-4]. As a result, removing antibiotics attracts a particular point of view on pollutant remediation.

Among the antibiotics, amoxicillin (AMX) is the second-line antibiotic for COVID-19 patients after doxycycline, suggested by National Institute for Health and Care Excellence (NICE) COVID-19 guidance [5]. Besides, AMX is also used to treat other diseases and in veterinary medicine. Due to the highly used and poorly metabolized (80–90% excreted by the body), AMX could be detected in the environment. AMX has been detected in the Eastern Mediterranean Sea up to 127.8 ng/L, the highest among other detected pharmaceuticals [6]. In addition, the Predicted Environmental Concentration (PEC) of AMX in the UK emergency hospital at Harrogate is 30 ng/L in the baseline river and 400 ng/L in the case of 95% of the patient prescribed antibiotics [5]. Conventional water treatment, such as filtration, cannot remove the AMX residue [3]. Therefore, the development of remediation techniques is urgently needed to treat antibiotic pollutants.

In recent years, advanced oxidation processes (AOPs) have been recognized as one of the promising techniques for antibiotic removal. AOPs use the in situ-generated strong oxidative species (H_2O_2, $OH^{\bullet}$, and $^{\bullet}O_2^-$) to degrade antibiotic compounds into harmless

substances [7–9]. Heterogeneous photocatalysis is the most popular AOPs method because of its effectiveness and environmentally friendly. The semiconductor is used for photocatalysis processes, and the photon induces the oxidation reaction [10].

The semiconductor that has been studied for photodegradation of AMX such as NiO [11], ZnO [12-13], and TiO_2 [14-15]. TiO_2 is one of the most used in AOPs owing to its photo and chemical stability, non-toxicity, and excellent photoactivity. However, the major drawback of TiO_2 is the wide band gap of 3.2 eV. Consequently, the photoactivity of TiO_2 is only possessed in the presence of UV light. The doping method has been studied to improve the TiO_2 activity under visible light irradiation by narrowing the band gap and shifting the absorption regions [16-17]. Doping with metal or non-metal to improve TiO_2 activity in visible or solar light for AMX degradation has been studied extensively [3,18-21].

Doping TiO_2 with metal could enhance the photocatalytic activity due to the lower band gap energy, and metal could act as an electron trapper that inhibits electron and hole recombination. However, metal doping could leach during the photocatalytic process; consequently, the catalyst would deactivate, and a second source of pollutants formed [22]. Meanwhile, non-metal doping is more environmentally friendly and lower cost compared to metal doping. The non-metal elements, such as nitrogen, carbon, and sulfur, could substitute oxygen in the TiO_2 lattice which leads to narrower band gap energy. Among other non-metal dopants, nitrogen-doped TiO_2 shows outstanding photocatalytic activity under visible light for organic compound degradation [23-24]. That is due to the 2p states of the nitrogen atom could be mixed with the 2p states of the oxygen atom, allowing the band gap to narrow; as a result, a red shift of the absorption band edge to the visible region [22,24-25].

Therefore, in this work, the nitrogen element was selected as the dopant element to improve the TiO_2 activity for AMX degradation under visible light radiation. The nitrogen was doped into TiO_2 by the sol-gel method. The effect of nitrogen initial doping concentration was also studied. Different characterization methods XRD, FTIR, UV-SRS, and SEM-EDX, were carried out to examine the optimum doping level. Importantly, the photodegradation process of AMX was conducted under commercially visible LED-light irradiation. To the best of our knowledge, the AMX degradation by N-doped TiO_2 compared to undoped TiO_2 under commercially LED-light irradiation without an additional oxidative agent has not been conducted.

■ EXPERIMENTAL SECTION

Materials

Titanium tetraisopropoxide (TTIP) ($C_{12}H_{28}O_4Ti$; 98%) was purchased from Shanghai Chemical Industry. Ethanol (C_2H_6O, 99.99%), nitric acid (HNO_3, 65%), and urea (CH_2N_2O) were supplied by Merck company. All the chemicals used in this work were analytical grade. Amoxicillin trihydrate ($C_{16}H_{25}N_3O_8S$) was provided by the National Agency of Drug and Food Control, Republic of Indonesia.

Instrumentation

The N-doped TiO_2 properties were studied using different characterization techniques. Fourier Transform Infra-Red (FTIR) spectrum of undoped and N-doped TiO_2 was obtained on Shimadzu Prestige21. The crystal structure of the photocatalysts was investigated using an X-ray diffractometer (Shimadzu 6000D) with Cu Kα radiation in the range of = 10–80° with a scan speed of 3°/min. The UV-Visible specular reflectance spectroscopy (UV-SRS) UV1700 Pharmaspec was used to obtain the absorption spectra. The surface morphology and element composition of the photocatalysts were observed by scanning electron microscope (SEM) (JSM-6510LA) and energy dispersive spectroscopy (EDS).

Procedure

Synthesis of N-doped TiO_2

N-doped TiO_2 (TiO_2-N) with different nitrogen amounts was synthesized by sol-gel method using TTIP 98% and urea as TiO_2 and nitrogen precursor. In a typical sol-gel synthesis, 2 mL of TTIP was dissolved in 10 mL of ethanol under continuous stirring for 30 min to prepare solution A. In a beaker, urea was dissolved in water and mixed with ethanol to form solution B. The

pH of the solution was adjusted to 3 with the addition of HNO_3. The weight of urea was controlled to get the N/TiO_2 mass ratio of 15, 30, and 45% (w/w). Later, solution B was added dropwise into solution A under continuous stirring for 1 h. The obtained white solution was left overnight at room temperature to complete the gel formation. After that, the gel was dried for 5 h at 80 °C to remove the excess solution. The dried gel was ground to form a fine powder. Lastly, the powder was calcined in a muffle furnace for 2 h at 500 °C. A yellowish powder was obtained after the calcination process. The undoped TiO_2 was also synthesized in a similar procedure without adding urea.

Photocatalytic degradation of amoxicillin

The AMX photodegradation process was conducted in a batch photoreactor under visible light irradiation using LED lamps (Philips, 4 × 18 W, 400–700 nm). The photocatalytic process under UV light was also evaluated using a UVA lamp (4 × 18 W, 320–400 nm). Firstly, a specific amoxicillin weight was diluted to get a 20 mg/L solution concentration. The N-doped TiO_2 (catalyst dosage 1 g/L) was dispersed into AMX solution followed by 1 h stirring in the dark to reach the adsorption equilibrium between the drug and the catalyst. Later, the solution was irradiated at specific time intervals. After each irradiation time, the AMX solution was separated from the catalyst by centrifugation. The remaining AMX in solution was analyzed at maximum wavelength absorption (227 nm) [26] using a UV-Visible spectrophotometer. The absorption spectrum of AMX is shown in Fig. 1. The percentage of AMX degradation was calculated using Eq. (1):

$$\% \text{ Dye degradation} = \frac{A_0 - A_t}{A_0} \times 100\% \quad (1)$$

where A_0 and A_t denote the AMX concentration before and after the degradation, respectively.

■ RESULTS AND DISCUSSION

X-ray Diffraction Analysis

The crystal structure of the photocatalyst was characterized by the X-ray diffraction method and presented in Fig. 2. The diffraction pattern for both

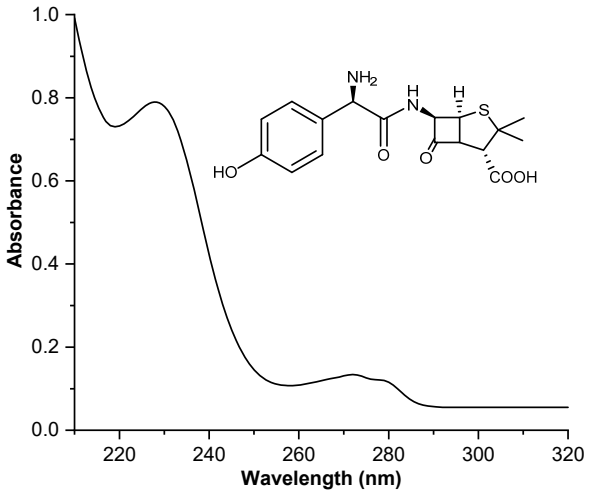

Fig 1. The UV absorption spectrum of amoxicillin

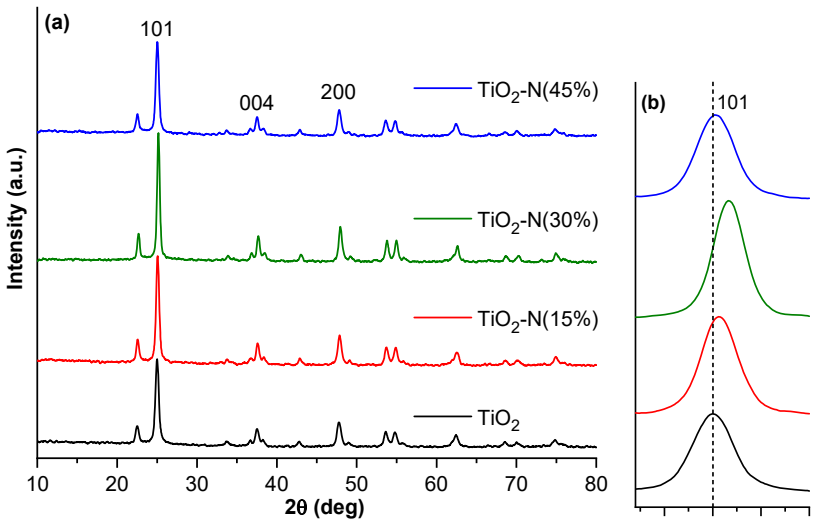

Fig 2. The X-ray diffraction patterns of N-doped and undoped TiO_2 in the range of 10–80° (a) and 24.25–26° (b)

undoped and N-doped TiO_2 are well-matched with the TiO_2 anatase (JCPDS card no. 21-1272). The anatase phase performs better photocatalytic activity compared to the rutile or brookite phase due to the larger surface area and better charge-carrier mobility [27-28]. Therefore, confirming the TiO_2 crystal structure for photocatalysis application is necessary. The peak of undoped TiO_2 observed at 2θ values of 25.00°, 37.57°, 47.79°, 53.65°, and 54.80° correspond to 101, 004, 200, 105, and 211 planes of the anatase phase. No new diffraction peaks were introduced in the N-doped TiO_2 diffractogram, which indicates that the N doping has not triggered the formation of any secondary and impurity phases of TiO_2 [23,29]. However, a positive shift of 101 peaks was observed for N-doped samples (Fig. 2(b)). The peak shift indicates the nitrogen has successfully doped into the TiO_2 lattice, engendered oxygen vacancies [30].

Moreover, the crystallinity of TiO_2 improved for the N-doped sample (15% and 30% doping levels), which may be the result of the doping nitrogen species. By applying Scherrer's equation, the average crystallite size was obtained. The increase in initial nitrogen concentration up to 30% leads to an increase in average crystallite size from 10.159 to 13.189 nm, as listed in Table 1. The incorporation of nitrogen into the TiO_2 lattice promotes the TiO_2 crystal growth [31-32]. On the other hand, at higher nitrogen doping levels (45%), the average crystallite size has slightly decreased, indicating enormous amounts of dopant had an inhibition effect on the crystal growth [33]. The N-doping on TiO_2 was well discovered by XRD analysis. FTIR analysis was performed to ensure nitrogen had successfully doped into the TiO_2.

FTIR Analysis

FTIR spectra displayed in Fig. 3 elucidate the surface functional group of undoped TiO_2 and N-doped TiO_2 at different amounts of nitrogen loading. All the samples present almost the same spectra at around 400–900, 1631, and broadband at 3449 cm^{-1}, which corresponds to the TiO_2 anatase phase. The absorption band at 400–900 cm^{-1} is assigned to the Ti–O–Ti stretching vibration, while the 1631 and 3449 cm^{-1} bands are attributed to O–H bending and O–H stretching vibration from Ti–O–H [34-35]. The

Table 1. The average crystallite size and band gap energy of N-doped and undoped TiO_2

Sample	Average crystallite size (nm)	Band gap (eV)
TiO_2	10.159	3.18
TiO_2-N (15%)	10.716	3.04
TiO_2-N (30%)	13.189	2.97
TiO_2-N (45%)	10.054	3.03

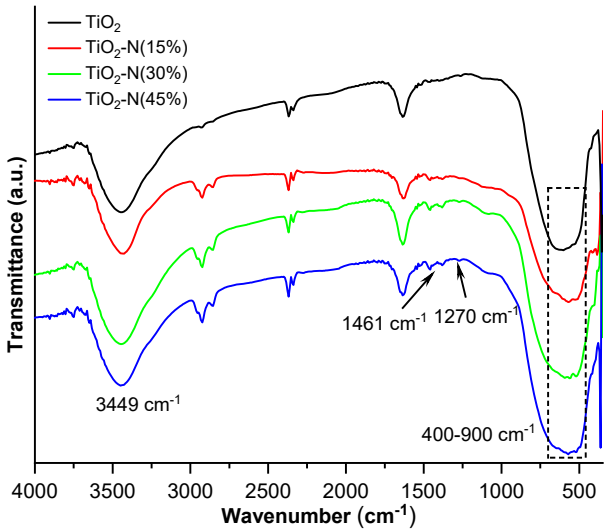

Fig 3. FTIR spectra of N-doped and undoped TiO_2

doped samples show notable bands at around 1461 and 1270 cm^{-1} correspond to the vibration of the N–Ti bond, which are the typical bands of N in the TiO_2 lattice [22,30,36-37]. The findings are in good agreement with the XRD analysis as discussed above.

UV-SRS Analysis

Incorporating nitrogen in TiO_2 could narrow the gap between the valance and conduction bands, and then improve the photocatalytic activity [23]. Those optical properties were investigated by UV-SRS, as shown in Fig. 4. It was observed that nitrogen doping contributed to the redshift because of the narrowing of the band gap. The edge of absorption spectra slightly shifts to the longer wavelength. Additionally, after doping with nitrogen, the absorption of the N-doped sample in the visible region rises. At a 30% doping level, the highest absorption was achieved. As predicted, this sample would give the lowest band gap energy of 2.97 eV. The narrowing of band gap energy could be

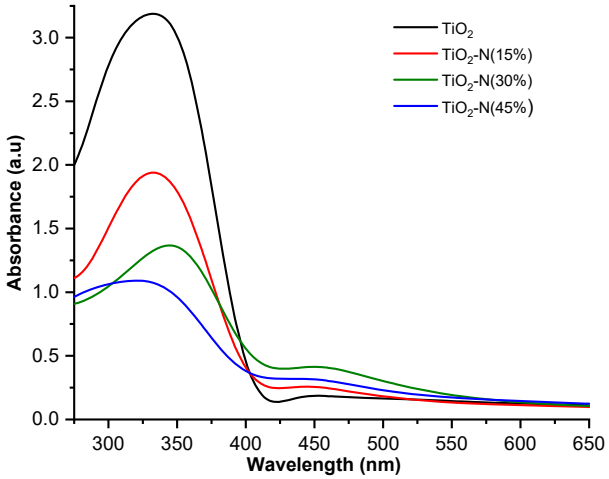

Fig 4. UV-SRS absorbance spectra of N-doped and undoped TiO_2

attributed to the submission of N instead of O in the TiO_2 lattice, creating a new energy level [22-24], which leads to the absorption of visible light and initiates photocatalysis as proposed in Fig. 9.

The band gap energy was determined using the Tauc plot and displayed in Fig. 5. The amount of nitrogen doping influences the redshift of light adsorption region and band gap energy. The higher nitrogen loading, the higher the absorption in the visible region and the lower the band gap. On the other hand, the incorporation of nitrogen into the TiO_2 lattice becomes ineffective at massive nitrogen levels, and crystal growth is inhibited. Hence, at a 45% doping level, the band gap was obviously higher than the 30% nitrogen doping level. This result was in accordance with the XRD analysis.

SEM-EDX Analysis

Fig. 6(a) and b present the morphology and surface composition of TiO_2-N (30%) by SEM-EDX. The N-doped TiO_2 particles were spherically shaped in nano size. No observations of particle agglomeration in the sample, which would be advantageous for the photocatalytic process. The EDX analysis verified the presence of nitrogen in the sample. The nitrogen content present in TiO_2 (0.12%) was drastically dropped compared to initial nitrogen concentrations (30%). The result agrees with the previous report that only a small amount of nitrogen is deposited into the TiO_2 lattice. Meanwhile, the particular nitrogen element presents as amine absorbed in TiO_2 and then decomposed during the heat treatment at 500 °C [25,30].

Photocatalytic Degradation of Amoxicillin

To confirm the photocatalytic activity of the N-doped and undoped TiO_2, the degradation processes of AMX have been conducted in both UV and visible light.

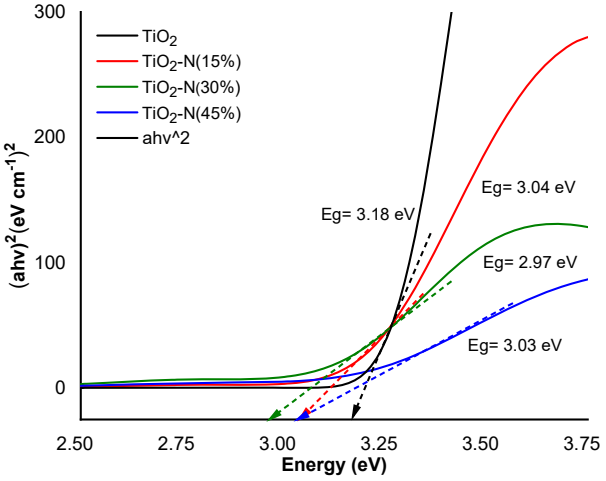

Fig 5. Tauc plot obtained from UV–SRS spectra of N-doped and undoped TiO_2

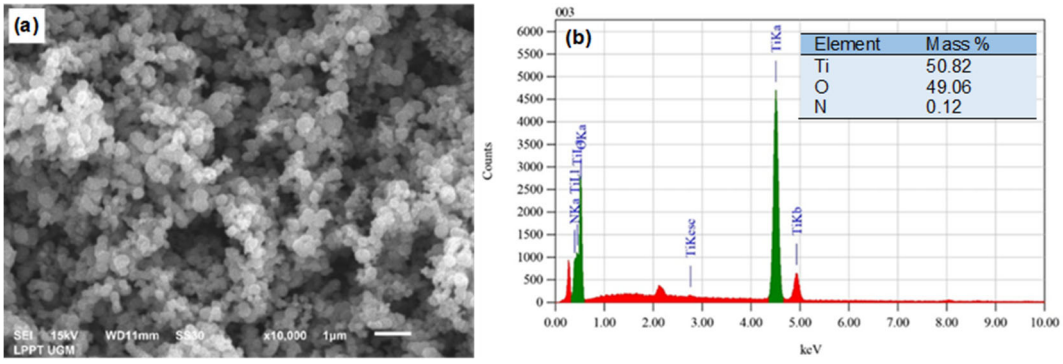

Fig 6. SEM image (a) and energy-dispersive spectra (b) of TiO_2-N(30%)

The result is exhibited in Fig. 7. The direct photolysis of AMX by visible light resulting 12.4% degradation after 300 min. Thus, confirming that the contribution of direct photolysis is quite low, even at longer light exposure. The finding was in accordance with the previous report. AMX is stable through photolysis by irradiation of light above the wavelength of 300 nm [38-40].

As predicted, the AMX degradation percentage by N-doped TiO_2 was higher than undoped TiO_2. The N-doped and undoped TiO_2 degradation percentages were 68.5 and 38.7%, respectively. The result has a good agreement with the characterization as discussed above, that the nitrogen doping at 30% initial dopant concentration has successfully incorporated in TiO_2, increased the absorption in the visible region, and narrowed the band gap energy (2.97 eV). Therefore, it is reasonable that N-doped TiO_2 exhibits higher photocatalytic activity under visible light irradiation compared to bare TiO_2. Moreover, the N-doped increased the degradation percentage to 84.12% compared to pure TiO_2 (78.01%) in UV irradiation. TiO_2 itself has good photocatalytic activity under UV irradiation, while the nitrogen dopant allows to a lower electron-hole recombination rate that enhances the TiO_2 activity [21,23].

The result is in accordance with the previous report [26,41-42] that the AMX could not completely degrade by TiO_2 or doped TiO_2. The removal of AMX at the first stage was due to the adsorption of AMX on the active site of the catalyst. While the radiation starts, the AMX starts to decompose by the oxidative species produced by the catalyst. However, at the longer time of light exposure, the degradation rate decreases and the AMX could not completely degrade. This can be caused by the saturated active site of the catalyst. Additionally, at the late stage, the oxidative species have been consumed to oxidize the AMX and hence the amount of oxidative species was not sufficient to degrade all the AMX molecules [41]. Despite that, nitrogen doping successfully increased the degradation of AMX by TiO_2 under visible light irradiation, which is more environmentally benign. Further study is required to increase the catalyst's active site and increase the number of oxidative species, so the pharmaceutical pollutant can completely decompose.

The progressive degradation of AMX by N-doped TiO_2 under visible light illumination is displayed in Fig. 8. The maximum wavelength of AMX solution is 227 nm. The maximum peak gradually decreased as the irradiation time increased and almost vanished after 300 min irradiation. No new absorption peak was observed during the degradation, indicating that other compounds

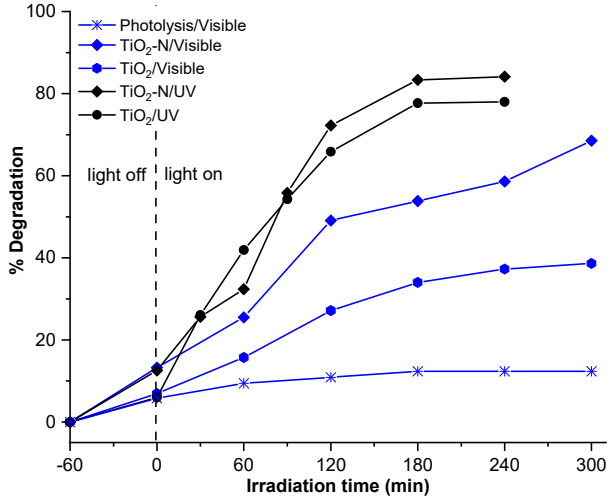

Fig 7. The AMX degradation by TiO_2 compared to TiO_2-N (30%) under UV and visible light irradiation ($[AMX]_0$ = 20 mg/L, catalyst dosage = 1 g/L)

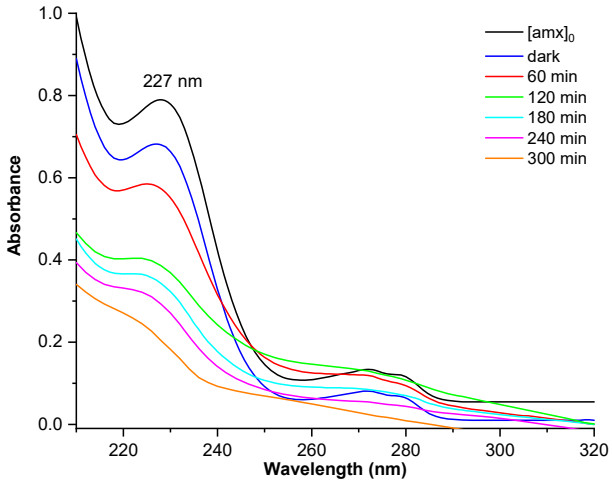

Fig 8. The changeover UV-Visible spectra of AMX before and after photodegradation by N-doped TiO_2 under visible light irradiation ($[AMX]_0$ = 20 mg/L, catalyst dosage = 1 g/L, irradiation time = 60–300 min)

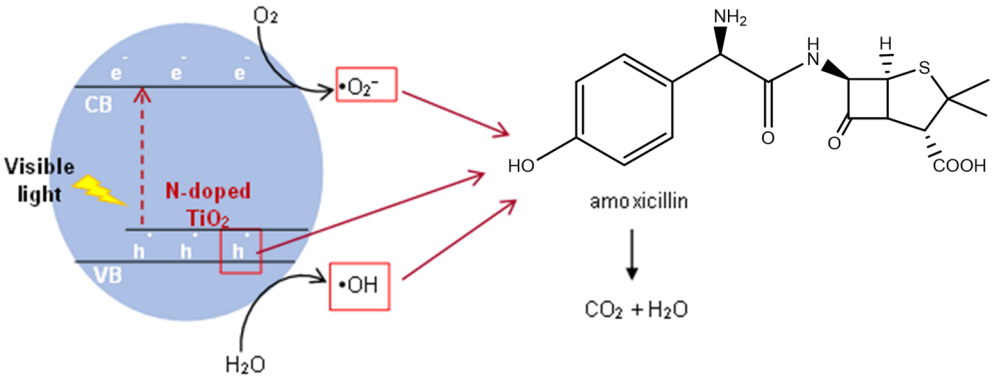

Fig 9. Proposed degradation mechanism of AMX by using N-doped TiO_2

or intermediates were not detected in this degradation process. The AMX degraded up to 68.5%, resulting in small molecules such as H_2O and CO_2. The proposed degradation mechanism of AMX by advanced oxidation process using N-doped TiO_2 is presented in Fig. 9. The nitrogen doping forms a new energy level between the valence and conduction band of TiO_2 and narrows the band gap [24-25]. Therefore, visible light irradiation is adequate to excite an electron from the valence band into the conduction band. The formation pairs of electrons (e^-) and holes (h^+) will initiate the production of oxidative species: $OH^•$ and $^•O_2^-$. The oxidative species (h^+, $OH^•$, and $^•O_2^-$) played an essential role in the degradation of AMX, then decomposed the compound into CO_2 and H_2O [3,19]. The proposed mechanism was adopted from the previous study [9,20,43-44].

■ CONCLUSION

The result of our study showed that initial nitrogen concentration affects the resulting N-doped TiO_2 catalyst. Nitrogen with an initial concentration of 30% (w/w) was successfully doped onto TiO_2 and had the lowest band gap energy of 2.97 eV. The presence of nitrogen increases the photodegradation of AMX for both UV and visible light irradiation. Nitrogen has narrowed the TiO_2 band gap energy that enhanced the TiO_2 activity under visible light for AMX degradation. AMX degraded 68.5% under visible light radiation, higher than bare TiO_2 (38.7%). Therefore, N-doped TiO_2 had good potential as a photocatalyst for the degradation of pharmaceutical pollutant under visible light irradiation in a natural aqueous solution without an additional oxidative agent.

■ ACKNOWLEDGMENTS

The authors acknowledge the financial support from the PMDSU scholarship by the Ministry of Research, Technology and Higher Education, Republic of Indonesia (Contract No. 3139/UN1.DITLIT/DIT-LIT/PT/2020).

■ AUTHOR CONTRIBUTIONS

Kusuma Putri Suwondo performed the experiment, analyzed the data, and wrote the article. Nurul Hidayat Aprilita contributed to supervise the data interpretation and revised the manuscript, and Endang Tri Wahyuni contributed to conceive the idea of this research, supervised the data interpretation, and revised the manuscript.

■ REFERENCES

[1] Center for Systems Science and Engineering (CSSE) at Johns Hopkins University, 2023, *COVID-19 Dashboard* [Updated 2023 January], https://coronavirus.jhu.edu/, accessed on January 10, 2023.

[2] Langford, B.J., So, M., Raybardhan, S., Leung, V., Soucy, J.P.R., Westwood, D., Daneman, N., and MacFadden, D.R., 2021, Antibiotic prescribing in patients with COVID-19: Rapid review and meta-analysis, *Clin. Microbiol. Infect.*, 27 (4), 520–531.

[3] Salimi, M., Behbahani, M., Sobhi, H.R., Gholami, M., Jonidi Jafari, A., Rezaei Kalantary, R., Farzadkia, M., and Esrafili, A., 2019, A new nano-photocatalyst based on Pt and Bi co-doped TiO_2 for

efficient visible-light photo degradation of amoxicillin, *New J. Chem.*, 43 (3), 1562–1568.

[4] Munguia, J., and Nizet, V., 2018, Pharmacological targeting of the host-pathogen interaction: Alternatives to classical antibiotics to combat drug-resistant superbugs, *Trends Pharmacol. Sci.*, 38 (5), 473–488.

[5] Comber, S.D.W., Upton, M., Lewin, S., Powell, N., and Hutchinson, T.H., 2020, COVID-19, antibiotics and one health: A UK environmental risk assessment, *J. Antimicrob. Chemother.*, 75 (11), 3411–3412.

[6] Alygizakis, N.A., Gago-Ferrero, P., Borova, V.L., Pavlidou, A., Hatzianestis, I., and Thomaidis, N.S., 2016, Occurrence and spatial distribution of 158 pharmaceuticals, drugs of abuse and related metabolites in offshore seawater, *Sci. Total Environ.*, 541, 1097–1105.

[7] Khan, A.H., Khan, N.A., Ahmed, S., Dhingra, A., Singh, C.P., Khan, S.U., Mohammadi, A.A., Changani, F., Yousefi, M., Alam, S., Vambol, S., Vambol, V., Khursheed, A., and Ali, I., 2020, Application of advanced oxidation processes followed by different treatment technologies for hospital wastewater treatment, *J. Cleaner Prod.*, 269, 122411.

[8] Cuerda-Correa, E.M., Alexandre-Franco, M.F., and Fernández-González, C., 2020, Advanced oxidation processes for the removal of antibiotics from water. An overview, *Water*, 12 (1), 102.

[9] Wang, J., and Zhuan, R., 2020, Degradation of antibiotics by advanced oxidation processes: An overview, *Sci. Total Environ.*, 701, 135023.

[10] Byrne, C., Subramanian, G., and Pillai, S.C., 2018, Recent advances in photocatalysis for environmental applications, *J. Environ. Chem. Eng.*, 6 (3), 3531–3555.

[11] Balarak, D., and Mostafapour, F.K., 2019, Photocatalytic degradation of amoxicillin using UV/Synthesized NiO from pharmaceutical wastewater, *Indones. J. Chem.*, 19 (1), 211–218.

[12] Elmolla, E.S., and Chaudhuri, M., 2010, Photocatalytic degradation of amoxicillin, ampicillin and cloxacillin antibiotics in aqueous solution using UV/TiO_2 and UV/H_2O_2/TiO_2 photocatalysis, *Desalination*, 252 (1-3), 46–52.

[13] Moradi, M., Hasanvandian, F., Isari, A.A., Hayati, F., Kakavandi, B., and Setayesh, S.R., 2021, CuO and ZnO co-anchored on g-C_3N_4 nanosheets as an affordable double Z-scheme nanocomposite for photocatalytic decontamination of amoxicillin, *Appl. Catal., B*, 285, 119838.

[14] Chinnaiyan, P., Thampi, S.G., Kumar, M., and Balachandran, M., 2019, Photocatalytic degradation of metformin and amoxicillin in synthetic hospital wastewater: Effect of classical parameters, *Int. J. Environ. Sci. Technol.*, 16 (10), 5463–5474.

[15] Dimitrakopoulou, D., Rethemiotaki, I., Frontistis, Z., Xekoukoulotakis, N.P., Venieri, D., and Mantzavinos, D., 2012, Degradation, mineralization and antibiotic inactivation of amoxicillin by UV-A/TiO_2 photocatalysis, *J. Environ. Manage.*, 98, 168–174.

[16] Xing, X., Du, Z., Zhuang, J., and Wang, D., 2018, Removal of ciprofloxacin from water by nitrogen doped TiO_2 immobilized on glass spheres: Rapid screening of degradation products, *J. Photochem. Photobiol., A*, 359, 23–32.

[17] Wetchakun, K., Wetchakun, N., and Sakulsermsuk, S., 2019, An overview of solar/visible light-driven heterogeneous photocatalysis for water purification: TiO_2- and ZnO-based photocatalysts used in suspension photoreactors, *J. Ind. Eng. Chem.*, 71, 19–49.

[18] Bergamonti, L., Graiff, C., Bergonzi, C., Potenza, M., Reverberi, C., Ossiprandi, M.C., Lottici, P.P., Bettini, R., and Elviri, L., 2022, Photodegradation of pharmaceutical pollutants: New photocatalytic systems based on 3D printed scaffold-supported Ag/TiO_2 nanocomposite, *Catalysts*, 12 (6), 580.

[19] Lalliansanga, L., Tiwari, D., Lee, S.M., and Kim, D.J., 2022, Photocatalytic degradation of amoxicillin and tetracycline by template synthesized nano-structured Ce^{3+}@TiO_2 thin film catalyst, *Environ. Res.*, 210, 112914.

[20] Çağlar Yılmaz, H., Akgeyik, E., Bougarrani, S., El Azzouzi, M., and Erdemoğlu, S., 2020, Photocatalytic degradation of amoxicillin using Co-doped TiO_2 synthesized by reflux method and

monitoring of degradation products by LC–MS/MS, *J. Dispersion Sci. Technol.*, 41 (3), 414–425.

[21] Mhemid, R.K.S., Salman, M.S., and Mohammed, N.A., 2022, Comparing the efficiency of N-doped TiO_2 and commercial TiO_2 as photo catalysts for amoxicillin and ciprofloxacin photodegradation under solar irradiation, *J. Environ. Sci. Health, Part A: Toxic/Hazard. Subst. Environ. Eng.*, 57 (9), 813–829.

[22] Gomes, J., Lincho, J., Domingues, E., Quinta-Ferreira, R.M., and Martins, R.C., 2019, N-TiO_2 photocatalysts: A review of their characteristics and capacity for emerging contaminants removal, *Water*, 11 (2), 373.

[23] Zhao, W., Liu, S., Zhang, S., Wang, R., and Wang, K., 2019, Preparation and visible-light photocatalytic activity of N-doped TiO_2 by plasma-assisted sol-gel method, *Catal. Today*, 337, 37–43.

[24] Asahi, R., Morikawa, T., Irie, H., and Ohwaki, T., 2014, Nitrogen-doped titanium dioxide as visible-light-sensitive photocatalyst: Designs, developments, and prospects, *Chem. Rev.*, 114 (19), 9824–9852.

[25] Nolan, N.T., Synnott, D.W., Seery, M.K., Hinder, S.J., Van Wassenhoven, A., and Pillai, S.C., 2012, Effect of N-doping on the photocatalytic activity of sol-gel TiO_2, *J. Hazard. Mater.*, 211-212, 88–94.

[26] Verma, M., and Haritash, A.K., 2020, Photocatalytic degradation of Amoxicillin in pharmaceutical wastewater: A potential tool to manage residual antibiotics, *Environ. Technol. Innovation*, 20, 101072.

[27] Hanaor, D.A.H., and Sorrell, C.C., 2011, Review of the anatase to rutile phase transformation, *J. Mater. Sci.*, 46 (4), 855–874.

[28] Odling, G., and Robertson, N., 2015, Why is anatase a better photocatalyst than rutile? The importance of free hydroxyl radicals, *ChemSusChem*, 8 (11), 1838–1840.

[29] Zhao, Z., Omer, A.A., Qin, Z., Osman, S., Xia, L., and Singh, R.P., 2019, Cu/N-codoped TiO_2 prepared by the sol-gel method for phenanthrene removal under visible light irradiation, *Environ. Sci. Pollut. Res.*, 27 (15), 17530–17540.

[30] Li, H., Hao, Y., Lu, H., Liang, L., Wang, Y., Qiu, J., Shi, X., Wang, Y., and Yao, J., 2015, A systematic study on visible-light N-doped TiO_2 photocatalyst obtained from ethylenediamine by sol-gel method, *Appl. Surf. Sci.*, 344, 112–118.

[31] Yang, G., Jiang, Z., Shi, H., Xiao, T., and Yan, Z., 2010, Preparation of highly visible-light active N-doped TiO_2 photocatalyst, *J. Mater. Chem.*, 20 (25), 5301–5309.

[32] Huo, Y., Jin, Y., Zhu, J., and Li, H., 2009, Highly active $TiO_{2-x-y}N_xF_y$ visible photocatalyst prepared under supercritical conditions in NH_4F/EtOH fluid, *Appl. Catal., B*, 89 (3-4), 543–550.

[33] Cheng, X., Yu, X., and Xing, Z., 2012, Characterization and mechanism analysis of N doped TiO_2 with visible light response and its enhanced visible activity, *Appl. Surf. Sci.*, 258 (7), 3244–3248.

[34] Liu, C., Yu, T., Tan, X., and Huang, X., 2017, Comparison N-Cu–codoped nanotitania and N-doped nanotitania in photocatalytic reduction of CO_2 under UV light, *Inorg. Nano-Met. Chem.*, 47 (1), 9–14.

[35] Reda, S.M., Khairy, M., and Mousa, M.A., 2020, Photocatalytic activity of nitrogen and copper doped TiO_2 nanoparticles prepared by microwave-assisted sol-gel process, *Arabian J. Chem.*, 13 (1), 86–95.

[36] Wang, H., Yang, X., Xiong, W., and Zhang, Z., 2015, Photocatalytic reduction of nitroarenes to azo compounds over N-doped TiO_2: Relationship between catalysts and chemical reactivity, *Res. Chem. Intermed.*, 41 (6), 3981–3997.

[37] Etacheri, V., Seery, M.K., Hinder, S.J., and Pillai, S.C., 2010, Highly visible light active $TiO_{2-x}N_x$ heterojunction photocatalysts, *Chem. Mater.*, 22 (13), 3843–3853.

[38] Bergamonti, L., Bergonzi, C., Graiff, C., Lottici, P.P., Bettini, R., and Elviri, L., 2019, 3D printed chitosan scaffolds: A new TiO_2 support for the photocatalytic degradation of amoxicillin in water, *Water Res.*, 163, 114841.

[39] Kanakaraju, D., Kockler, J., Motti, C.A., Glass, B.D., and Oelgemöller, M., 2015, Titanium dioxide/zeolite integrated photocatalytic

adsorbents for the degradation of amoxicillin, *Appl. Catal., B*, 166-167, 45–55.

[40] Moreira, N.F.F., Orge, C.A., Ribeiro, A.R., Faria, J.L., Nunes, O.C., Pereira, M.F.R., and Silva, A.M.T., 2015, Fast mineralization and detoxification of amoxicillin and diclofenac by photocatalytic ozonation and application to an urban wastewater, *Water Res.*, 87, 87–96.

[41] Gar Alalm, M., Tawfik, A., and Ookawara, S., 2016, Enhancement of photocatalytic activity of TiO_2 by immobilization on activated carbon for degradation of pharmaceuticals, *J. Environ. Chem. Eng.*, 4 (2), 1929–1937.

[42] Klauson, D., Babkina, J., Stepanova, K., Krichevskaya, M., and Preis, S., 2010, Aqueous photocatalytic oxidation of amoxicillin, *Catal. Today*, 151 (1-2), 39–45.

[43] Wahyuni, E.T., Yulikayani, P.Y., and Aprilita, N.H., 2020, Enhancement of visible-light photocatalytic activity of Cu-doped TiO_2 for photodegradation of amoxicillin in water, *J. Mater. Environ. Sci.*, 11 (4), 670–683.

[44] Nguyen, T.L., Pham, T.H., Viet, N.M., Thang, P.Q., Rajagopal, R., Sathya, R., Jung, S.H., and Kim, T., 2022, Improved photodegradation of antibiotics pollutants in wastewaters by advanced oxidation process based on Ni-doped TiO_2, *Chemosphere*, 302, 134837.